

RSC Advances



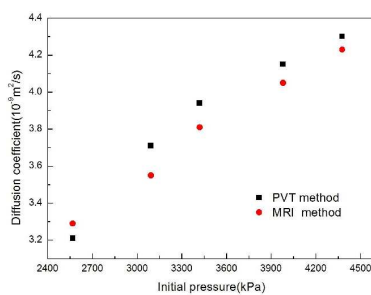
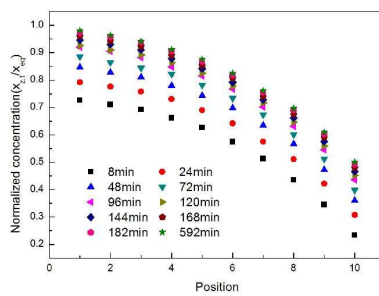
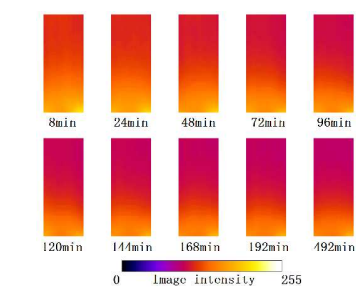
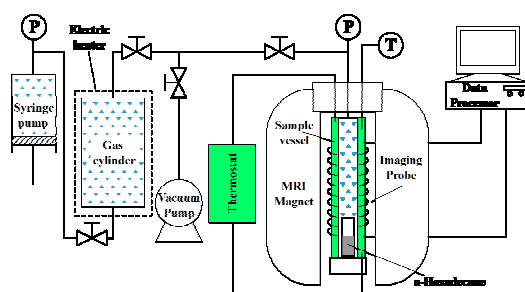
This is an *Accepted Manuscript*, which has been through the Royal Society of Chemistry peer review process and has been accepted for publication.

Accepted Manuscripts are published online shortly after acceptance, before technical editing, formatting and proof reading. Using this free service, authors can make their results available to the community, in citable form, before we publish the edited article. This *Accepted Manuscript* will be replaced by the edited, formatted and paginated article as soon as this is available.

You can find more information about *Accepted Manuscripts* in the [Information for Authors](#).

Please note that technical editing may introduce minor changes to the text and/or graphics, which may alter content. The journal's standard [Terms & Conditions](#) and the [Ethical guidelines](#) still apply. In no event shall the Royal Society of Chemistry be held responsible for any errors or omissions in this *Accepted Manuscript* or any consequences arising from the use of any information it contains.

Graphical Abstract



MRI was used to study the diffusion of CO₂ in n-hexadecane, and the overall diffusion coefficient was obtained.

CO₂ Diffusion in *n*-Hexadecane Investigated Using Magnetic Resonance Imaging and Pressure Decay Measurements

Yongchen Song¹, Min Hao^{1,2}, Yu Liu¹, Yuechao Zhao^{1,*}, Bo Su¹, and Lanlan Jiang

¹Key Laboratory of Ocean Energy Utilization and Energy Conservation of Ministry of Education, Dalian University of Technology, Dalian 116024, PR China

²School of Energy and Power Engineering, Shenyang University of Chemical Technology, Shenyang, Liaoning 110142, PR China

* Author to whom correspondence should be addressed; E-Mail: zhaoyc@dlut.edu.cn; Tel.: +86-411-84708015

Abstract: A method combining magnetic resonance imaging (MRI) and dual-chamber pressure decay (i.e., the pressure–volume–temperature method) was used to measure the diffusivity of CO₂ in bulk *n*-hexadecane, a representative oil, at 21 °C. Images of the proton density of *n*-hexadecane were obtained by MRI using a high magnetic field and high resolution, and the pressure decay was recorded. Overall diffusion coefficients of CO₂ were calculated from both pressure decay and MRI intensity data. The two results showed good agreement. MRI was successfully used to study the diffusivity of CO₂ in *n*-hexadecane. The change of image density (i.e., proton density) demonstrates that the oil density decreases as CO₂ diffuses into it. The finite volume method was applied to the images obtained by MRI, allowing the diffusion coefficient of CO₂ to be directly obtained. MRI methods can measure the unsteady-state local diffusion coefficient and overall diffusion coefficient of such systems.

Keywords: MRI; Image intensity; Pressure decay; CO₂; *n*-Hexadecane; Diffusivity

1 Introduction

Two miscible fluids will diffuse into each other when they come into contact. The molecular transport of one substance relative to another is known as diffusion. Diffusion plays an important role in the mixing of CO₂ and crude oil after injection of CO₂ into an oil reservoir.

CO₂-enhanced oil recovery (CO₂-EOR) has proven to be effective for improving domestic oil production. Moreover, use of CO₂ in oil recovery also provides considerable capacity for CO₂ mitigation [1]. The viscosity of oil can be lowered significantly by diffusion of CO₂ into it; thus, the mobility of oil in a reservoir can be improved [2]. Mass transfer between CO₂ and oil, which is mainly controlled by diffusivity, is the first mechanism that occurs during the CO₂-EOR process [3,4]. To describe this process quantitatively, the diffusion coefficient of CO₂ gas in oil needs to be determined.

Experimental methods used to measure the diffusivity of gas in oil can be broadly divided into two types: direct and indirect. The direct measurement of diffusivity is time consuming and involves measuring the change of concentration over time [5]. Indirect methods involve measuring the change of a parameter related to diffusion over time, such as volume, density or pressure [6,7]. The pressure decay method is a typical indirect method used to measure diffusivity. Riazi et al. [8] reported a pressure decay method using a pressure–volume–temperature (PVT) cell. In their experiment, both the position of the gas/liquid interface and gas pressure decay in the PVT cell were monitored during the diffusion process. Zhang et al. [9] measured the diffusion coefficient of CO₂ in heavy oils using a similar experimental method except that the position of the interface was considered constant. They also presented a nonlinear regression method that allowed the diffusion coefficient to be obtained directly from pressure decay data. Recently, non-intrusive detection methods such as X-ray computed tomography (CT) and magnetic resonance imaging (MRI) have been extended to the

area of petroleum research. Liu et al. [10] observed the miscible and immiscible CO₂ displacement of *n*-decane in glass-bead packed beds using an MRI scanner under high magnetic field. Residual oil saturation was quantitatively measured by intensity analysis of magnetic resonance (MR) images. Song et al. [11] determined the minimum miscible pressure of CO₂ and *n*-decane by the MRI method, and their results agreed well with previous data obtained with traditional methods. Meanwhile, X-ray CT has been used to measure density distribution in heavy oil and hydrocarbon solvent mixing experiments [12-14]. In these experiments, concentration profiles were obtained from CT images based on the relationship between bulk density and CT image intensity. Other researchers have used MRI to observe mass-transfer processes. Fisher et al. [15] used MRI to observe vapor extraction processes. They performed bitumen and heavy-oil vapor extraction experiments using butane and propane as solvents in dry sand and sand with connate water. In their experiments, the MRI signal, which corresponded to the oil saturation, provided not only the position of the vapor chamber but also concentration gradients.

The main objective of the present study is to use MRI technology to measure gas diffusion coefficients in oils, and investigate diffusion and mass transfer processes *in situ*. Diffusion coefficients of CO₂ in *n*-hexadecane are determined by measuring the pressure in a dual-chamber PVT system. MRI with high spatial resolution is used to observe the concentration distribution of CO₂ during diffusion. In addition, pressure data are recorded to calculate the molar mass of CO₂ diffusing into *n*-hexadecane. Pressure decay analysis is performed to calculate the steady-state diffusion coefficient of CO₂ in *n*-hexadecane. This study helps us to understand the diffusion behavior of CO₂ in a representative oil, so it will provide useful information for several oil recovery processes.

2 Experimental Details

2.1 Apparatus and Materials

An experimental system containing a gas cylinder and vessel for the MRI sample was constructed to measure the diffusion coefficient of CO₂ into a representative oil, *n*-hexadecane, using both the pressure decay method and MRI [10]. A schematic diagram of the experimental apparatus is shown in Fig. 1. The gas cylinder is a constant-volume (500-mL) stainless steel cylinder that is wrapped with an electric heater. The self-designed MRI sample vessel (Fig. 2) is made of polyimide to hold the diffusion samples at high pressure (up to 12.0 MPa). The sample vessel contained three main types of components: an inner tube with an inner diameter of 15 mm and wall thickness of 4.5 mm, an outer tube with an outer diameter of 38 mm, and inlet and outlet connectors. The outlet was blocked in the experiments. The temperature of the sample in the vessel was controlled by a circulator (F-25ME, Fluorinert™, Julabo, Inc., Seelbach, Germany) with a temperature control range of -45 to 200 °C and precision of ±0.5 °C. Inert liquid Fluorinert™ FC-40 was used as the temperature-control medium of the imaging vessel because it does not contain hydrogen atoms and thus has no influence on ¹H nuclear imaging. The gas cylinder and sample vessel formed a dual-chamber system, which can improve the pressure stability and measurement precision relative to those of a single-chamber system.

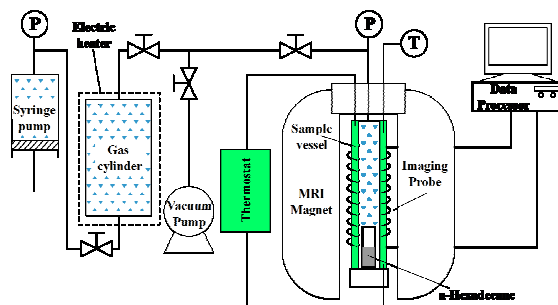


Fig. 1 Schematic diagram of the experimental apparatus

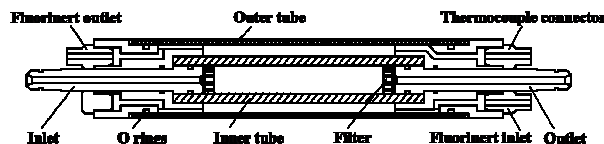


Fig. 2 Vertical-section diagram of the sample vessel

Images were measured using a 400-MHz NMR spectrometer (Varian Inc., Palo Alto, CA, USA) with microimaging kits including a 55-mm i.d. gradient coil, which provided a maximum gradient magnetic field of 50 Gauss/cm, and a 40-mm i.d. 400-MHz ^1H Millipede vertical imaging probe. All data and images were processed with a data processor.

N-Hexadecane of 98% purity was contained in a glass vial (i.d. = 8.8 mm) placed at the bottom of the sample vessel. Gaseous CO_2 of 99.99% purity was injected *via* a syringe pump into the gas cylinder to attain the desired pressure.

2.2 Procedure

Prior to performing experiments, the diffusion cell and all connections were pressurized with nitrogen and tested for leakage at pressures up to 8 MPa for at least 24 h.

All experiments were performed at 21 °C. The glass vial was filled to a height of about 20 mm with *N*-hexadecane. The system was placed under vacuum to extract air. After careful tuning, shimming and setting of the pulse parameters, the oil sample was scanned to obtain an initial MR image. CO_2 was then injected into the gas cylinder with the syringe pump until the desired pressure was reached. The pressure in the gas cylinder was set between 3000 and 5000 kPa. The gas valves were then turned on to allow CO_2 to enter the sample vessel and diffuse into the oil. The pressure was automatically recorded at the same time. Proton density images of the longitudinal planes along the diffusion direction were obtained while the pressure was being plotted. Each experiment was stopped after the pressure maintained a constant value (equilibrium

pressure) for 1 h. When the experiment had finished, the system was slowly depressurized to atmospheric pressure, dismantled and cleaned before starting a new experiment.

The steps of applying MRI into diffusion experiment imaging are as follows:

(1) Put the n-hexadecane-containing glass vials upright in the sample vessel, and keep the height consistent with the imaging probe.

(2) Debug the MRI analyzer; open Vnmrj in the image acquisition computer, and enter “tune” into the dialog box; tune by regulating the knobs "tune" and "match" below the probe; then start to shim: click “manual shim” on the “start” interface, entering the shimming interface; regulate by using the right and left mouse buttons, until the images are appropriate.

(3) Setting of parameters. All images were acquired with a standard spin-echo multi-slice (SEMS) pulse sequence, because this sequence is free from the impacts of main magnetic field inhomogeneity, and produces high-quality images. The specific imaging parameters are as follows: echo time (TE) = 4.9 ms, repetition time (TR) = 5 s, image data matrix = 96 pixels × 96 pixels, field of view (FOV) = 40 × 40 mm², slice thickness = 2 mm.

(4) Image acquisition. After gas injection was started, the MRIs were continuously acquired, until the end of the experiment.

2.3 Mathematical analysis

The diffusion process may be analyzed as shown in Fig. 3. This analysis can be derived based on the following assumptions [9,16,17]:

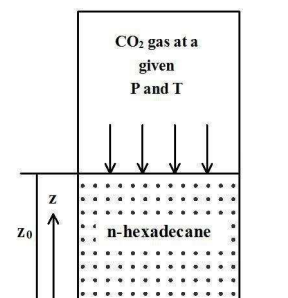


Fig. 3 Schematic diagram of the diffusion model

(1) The swelling height of the oil is negligible, that is, z_0 remains constant during the experiments.

(2) The temperature remains constant.

(3) The volatilization of *n*-hexadecane is negligible.

(4) The diffusion coefficient, D , does not change markedly with concentration during the experiments.

(5) The gas phase is a pure (single-component) gas.

The diffusion process can be expressed by Fick's law [9]:

$$\frac{dx}{dt} = D \frac{d^2x}{dz^2} \quad (1)$$

where x is the molar concentration of the gas at position z and time t , D is the diffusion coefficient.

Based on this hypothesis and combined with Fick's law, the relationship between pressure P and time t can be acquired using semi-infinite boundary conditions and the matter balance principle. When the higher-order terms were ignored, a 2-order analytical expression was obtained as follows [9]:

$$P(t) = m_1 \exp\left(-\frac{t}{k_1}\right) + m_2 \exp\left(-\frac{t}{k_2}\right) + P_{eq} \quad (2)$$

The first exponential term in Eq. (2) fits the main part of the pressure–time curve (large k) and the second term fits the initial part of the pressure–time curve during the incubation period (small k). Numerical fitting is required to obtain the values of m_1 , m_2 , k_1 , k_2 and P_{eq} . Because the incubation period is relatively short, the first exponential term is more suitable to calculate the integral diffusion coefficient. The diffusion coefficient D is then given by [9]:

$$D = \frac{4z_0^2}{k^* \pi^2} \quad (3)$$

where k^* is the greater of k_1 and k_2 , z_0 is the liquid surface height of n-hexadecane.

2.4 MR image analysis

An MR image of the proton density of *n*-hexadecane was obtained after one MRI scan. A region of interest (ROI) in the image was selected to analyze the diffusion process. Each ROI was 20-mm high, 7-mm wide and divided into ten segments of equal height. The image intensity of each segment at different times (defined as $I_{z,t}$) was then calculated. The initial I_0 (at $t = 0$) and final I_{eq} (at $t = t_{eq}$) values are constant at all positions.

CO₂ has no signal in MRI. A previous study [18] confirmed that the MR signal intensity at any location is proportional to the content of oil. When CO₂ diffuses into the oil, the content of oil decreases. Thus, the signal intensity of the MR images will weaken as the concentration of CO₂ increases. Therefore, the distribution of dimensionless CO₂ concentration can be calculated based on the measured signal intensity distribution of the MR images at each time period. According to Fick's law, the diffusion coefficients related to time and displacement can be computed based on such dimensionless concentrations. The concentration of CO₂ is related to the MR signal intensity. The normalized concentration of CO₂ in oil at different positions, z , and times, t , can be written as:

$$\frac{x_{z,t}}{x_{eq}} = \frac{I_0 - I_{z,t}}{I_0 - I_{eq}} \quad (4)$$

where $x_{z,t}$ represents the CO₂ concentration at position z and time t . I_0 represents the intensity at $t=0$, $I_{z,t}$ represents the intensity at time t and position z , and I_{eq} represents the intensity at $t=t_{eq}$. According to Zhao et al. [18], the concentration of CO₂ is related to MRI intensity. So we can then obtain the following:

$$x_{z,t} = k(I_0 - I_{z,t}) \quad (5-a)$$

$$x_0 = 0 \quad (5-b)$$

$$x_{eq} = k(I_0 - I_{eq}) = const \quad (5-c)$$

where k is a constant.

Here, a non-iterative, finite-volume analytical technique was used to calculate the diffusion coefficient of CO₂ in oil (*N*-hexadecane). It was assumed that there was a small composition gradient in the oil along the diffusion direction, and that the diffusion front did not move appreciably. Thus, Fick's Law (Eq. 1) can be used to relate the concentration and diffusion coefficient.

As shown in Fig. 4, the medium domain was discretized with mesh size Δz , time step Δt and grid points $z_i = i \times \Delta z$ ($i=1, 2, \dots, 10$) and $t_n = n \times \Delta t$ ($n=0, 1, 2, \dots$) [19-20].

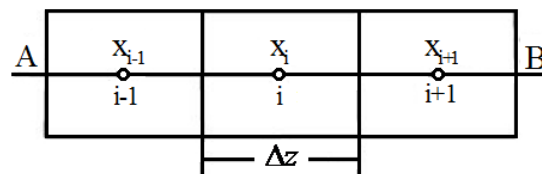


Fig. 4 Model of the finite-volume analytical method used in this work

Assuming that the concentration in boundary A is constant and there is no flux in boundary B , the discretized equations are as follows:

Internal points

$$-(x_i^n - x_{i-1}^n)D_{i-1/2}^n + (x_{i+1}^n - x_i^n)D_{i+1/2}^n = \frac{\Delta z^2}{\Delta t}(x_i^{n+1} - x_i^n) \quad (6-a)$$

Boundary A

$$-2(x_i^n - x_A^n)D_A^n + (x_{i+1}^n - x_i^n)D_{i+1/2}^n = \frac{\Delta z^2}{\Delta t}(x_i^{n+1} - x_i^n) \quad (6-b)$$

Boundary B

$$-(x_i^n - x_{i-1}^n)D_{i-1/2}^n + 2(x_B^n - x_i^n)D_B^n = \frac{\Delta z^2}{\Delta t}(x_i^{n+1} - x_i^n) \quad (6-c)$$

By arranging the discretized equations within the medium domain and at the boundary surfaces, Eq. (6) can be written in matrix form as $Ax = b$. Vector b is composed of the concentration measurement at specified grid locations along the sample in the experiment. The components of vector x are the unknown diffusion coefficients.

3 Results and Discussion

The pressure attenuation curves obtained with an initial pressure of 4377 kPa are shown in Fig. 5. A biexponential decrease in pressure is observed. Initially, the decrease was more pronounced, and became stable after an extended period. The decrease of pressure resulted from the dissolution of CO_2 , which demonstrates that the mass transfer rate during the initial stage of the experiment was relatively high. This suggests that high concentration and density gradients existed along the internal diffusion direction for n -hexadecane, which led to considerable convection and mass transfer. The initial stage of this high-mass-transfer diffusion is called the

"incubation period" [21]. With lengthening diffusion time, the internal concentration gradient and density gradient of hexadecane were gradually reduced. At the same time, the rates of mass transfer and pressure decay decreased. This result also indicates that after a long time, normal diffusion behavior occurs, and that mass transfer after the incubation period is dominated by molecular diffusion. Furthermore, it was found that a higher initial pressure resulted in a higher pressure decay rate and equilibrium being reached in less time than a lower initial pressure. It is evident that the incubation period has a considerable influence on the diffusion of CO₂, and a high initial pressure increases this influence.

The collected pressure–time data were numerically fitted in Origin with an accuracy of 0.974–0.993. The overall diffusion coefficient of CO₂ in *n*-hexadecane can be obtained by the fitted k^* using Eq. (3). The overall diffusion data obtained under different pressures are listed in Table 1. we calculated that the overall diffusion coefficient of CO₂ in *n*-hexadecane to be about $3.21\text{--}4.30\times 10^{-9}\text{ m}^2\text{ s}^{-1}$. Even though the exact experimental conditions used in the present work have not been used before, Wang et al. [22] and Grogan [23] obtained diffusion coefficients of $3.32\text{--}5.71\times 10^{-9}\text{ m}^2\text{ s}^{-1}$ and $1.8\text{--}3.21\times 10^{-9}\text{ m}^2\text{ s}^{-1}$, respectively, under similar conditions. Our diffusion coefficients are of the same order of magnitude as these.

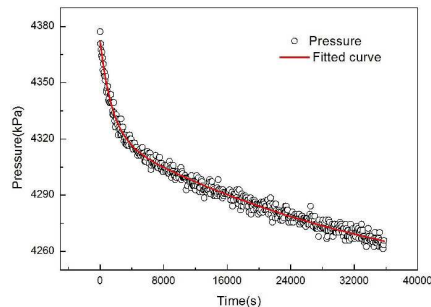


Fig. 5 Pressure decay during diffusion of CO₂ in *n*-hexadecane starting with an initial pressure of 4377kPa

Table 1 Pressure decay data for CO₂ diffusion in *n*-hexadecane at 21 °C

NO.	Oil height (mm)	Pressure of gas cylinder (kPa)	Initial pressure (kPa)	k^* (s)	D ($10^{-9}/\text{m}^2 \cdot \text{s}^{-1}$)
1	20	3000	2568	50537.3	3.21
2	20	3500	3093	49201.1	3.71
3	20	4000	3420	41170.2	3.94
4	20	4600	3980	39020.2	4.15
5	20	5000	4377	37680.5	4.30

The ROIs of MR images were cropped with image processing software. As an example, Fig. 6 shows a time series of ROIs of the diffusion process of CO₂ in *n*-hexadecane starting with an initial pressure of 4377 kPa. As CO₂ diffuses into *n*-hexadecane, a decrease in image intensity from top to bottom can be clearly observed because CO₂ is invisible in MR images. The CO₂ concentration distribution can be calculated from the image intensity data.

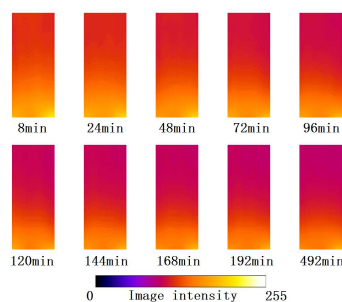


Fig. 6 Series of ROI images at different times during the CO₂ diffusion process for an initial pressure of 4377 kPa

The normalized concentration distribution of CO₂ along the diffusion direction at different times calculated by Eq. (4) for an initial pressure of 4377 kPa is shown in Fig. 7. Along the diffusion direction, the concentration of CO₂ decreases gradually. For a given diffusion distance, the concentration of CO₂ increases with time, which is consistent with the experimental results of Islas et al. [24].

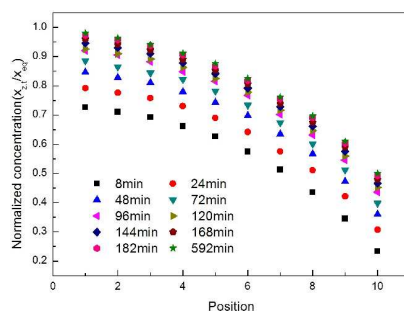
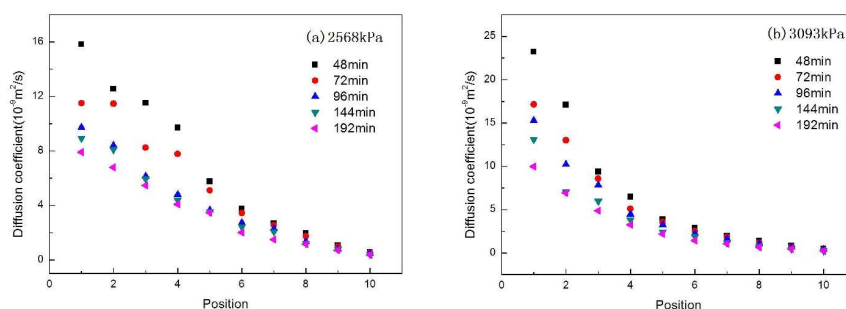


Fig. 7 Normalized CO₂ concentration distributions calculated from MR images with an initial pressure of 4377 kPa

The diffusion coefficients calculated from Eq. (6) for initial pressures of 2568, 3093, 3420, 3980 and 4377 kPa are depicted in Fig. 8. All of the diffusion coefficients decreased as the diffusion distance increased. Moreover, the diffusion coefficients decreased dramatically near the gas/oil interface and gradually decreased to a stable value as the diffusion distance increased. The maximum diffusion coefficient was observed near the interface, indicating that concentration and density gradients exist in *n*-hexadecane during dissolution and diffusion of CO₂. In addition, because the dissolution of CO₂ is much higher at the gas/oil interface, the concentration gradient at this interface is relatively high, which causes convection and results in increased diffusion. Furthermore, Fig. 8 also reveals that the diffusion coefficient in a given region decreases over time, which suggests that the influence of the density gradient on convection and the incubation period decreases. In addition, diffusion coefficients increase with increasing initial pressure, which is consistent with the findings of the pressure decay method.



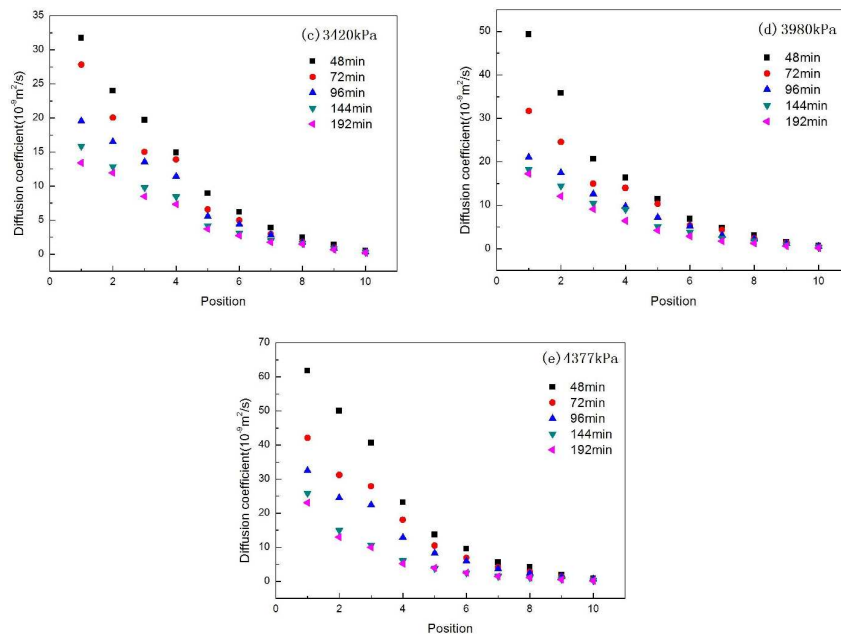


Fig. 8 Diffusion coefficients measured at different diffusion distances and times for initial pressures of (a) 2568 kPa, (b) 3093 kPa, (c) 3420 kPa, (d) 3980 kPa and (e) 4377 kPa

MRI can be used to measure the overall diffusion coefficient of CO_2 in *n*-hexadecane. The overall diffusion coefficient is the average of diffusion coefficients measured during the time it takes for diffusion to reach equilibrium. First, the computational time step was determined, and then the distribution of dimensionless CO_2 concentration was calculated using Eq. (4). The position dependence of diffusion coefficients was computed using Eq. (6). According to the relationship between diffusion coefficient and position, the trapezoidal rule was used to obtain the averages that represent time-dependent diffusion coefficients. Likewise, considering the relationship between diffusion coefficient and time, the trapezoidal rule was then used to average values to calculate the overall diffusion coefficient for each initial pressure. Fig. 9 shows the overall diffusion coefficients for different initial pressures calculated from the experimental MRI data and by the PVT method. According to Eq. (3), the error between the MRI and PVT is about

1.6–4.3%. The two results showed good agreement. MRI can measure both unsteady-state local diffusion coefficients and overall diffusion coefficients. In addition, According to the experimental results, the overall diffusion coefficients increase along with the increase of the initial pressure.

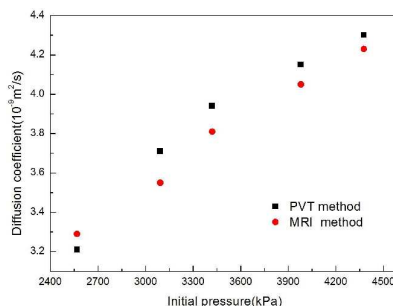


Fig. 9 Overall diffusion coefficients obtained by MRI and the PVT method

4 Conclusions

This study demonstrates that visualization and qualitative analysis of CO₂ diffusion in *n*-hexadecane can be achieved by combining MRI with the dual-chamber pressure decay method. The non-iterative finite-volume analytical technique can be used to calculate CO₂ diffusion coefficients from concentration profiles obtained from MR images. The results agree very well with the conventional pressure decay method in binary mixtures. MRI can determine both unsteady-state local diffusion coefficients and overall diffusion coefficients. Based on our experimental results, the following conclusions can be drawn:

- (1) The concentration of CO₂ decreases along the diffusion direction and is higher during the later stages of the reaction than during the initial stages.
- (2) The diffusion coefficient of CO₂ is a function of both diffusion time and diffusion distance. The diffusion coefficient decreases as diffusion distance and time increase

until an equilibrium state is reached.

- (3) The initial pressure has an obvious effect on the diffusion coefficient of CO₂, with pressure being directly proportional to diffusion coefficient.
- (4) The influence of the incubation period decreases with increasing diffusion time.

Mass transfer after the incubation period is mainly governed by molecular diffusion.

Acknowledgments

This study was supported by the National Natural Science Foundation of China (Grant No. 51206018, and 51106019), the National Basic Research Program of China (973) Program (Grant No. 2011CB707300), the National High Technology Research and Development of China (863) Program (Grant No. 2009AA63400), the Fundamental Research Funds for the Central Universities, the Specialized Research Fund for the Doctoral Program of Higher Education (Grant No. 20120041120057), the PhD Startup Foundation of Liaoning Province (Grant No. 20121022), and the Fundamental Research Funds for Central Universities (Grant No. DUT11RC(3)65, and DUT13LAB21).

Nomenclature

D	Diffusion coefficient (m ² /s)
$P(t), P_{eq}$	Measured and equilibrium pressure, respectively (kPa)
t	Time (s)
$x_{eq(P)}$	Oil-gas interface molar concentration at a given time (mol/cm ³)
z_0	Height of the oil in the vessel (cm)
$x_{z,t}$	CO ₂ concentration at position z and time t from MRI images

x_{eq}	CO ₂ concentration at equilibrium state
I_0	Initial image intensity at time $t = 0$
$I_{z,t}$	Image intensity at position z and time t
I_{eq}	Image intensity at equilibrium state
x	Molar concentration of CO ₂ gas

References

1. C.F.Robert, N. Christopher, V. L.Kuuskaa,“Storing CO₂ with enhanced oil recovery”, Energy Procedia, 1, 1989-1996 (2009)
2. M. Nobakht, S.Moghadam, and Y. Gu.,“Effects of Viscous and Capillary Forces on CO₂ Enhanced Oil Recovery under Reservoir Conditions”,Energy & Fuels.,21, 3469-3476 (2007)
3. Y. P. Zhang, C. L. Hyndman and B. B. Maini, “Measurement of gas diffusivity in heavy oils”, Journal of petroleum science and Engineering, 25, 37-47(2000)
4. A. Boustani,B.B. Maini, “The role of diffusion and convective dispersion in vapour extraction process”, J Canad Petrol Technol,No.4,40,68-77(2001)
5. J.C.Moulu, “Solution-gas drive:experiments and simulation”, J PetrolSciEng,No.4,2, 379-386(1989)
6. H. Sheikha,D.M. Pooladi,A.K. Mehrotra, “Development of graphical methods for estimating the diffusivity coefficient of gases in bitumen from pressure-decay data”,No.5,19, 2041-2049(2005)

7. P. Guo, Z. H.Wang, P. P. Shen and J. F. Du, “Molecular diffusion coefficients of the multicomponent gas-crude oil systems under high temperature and pressure.”,Industrial & Engineering Chemistry Research,No.19,48, 9023-9027(2009)
8. M.R.Riazi, “A new method for experimental measurement of diffusion coefficients in reservoir fluids”,Journal of Petroleum Science and Engineering,No.14, 235-250(1996)
9. Y.P. Zhang, C.L. Hyndman, B.B. Maini, “Measurement of gas diffusivity in heavy oils”,Journal of Petroleum Science and Engineering,25,37-47(2000)
10. Y. Liu, Y. Zhao, J. Zhao, Y. Song. “Magnetic resonance imaging on CO₂ miscible and immiscible displacement in oil-saturated glass beads pack.”,Magnetic Resonance Imaging.,No.29,1110-1118(2011)
11. Y. Song, N. Zhu, Y. Liu, J. Zhao, W. Liu, Y. Zhang , Y. Zhaoand L. Jiang,“Magnetic resonance imaging study on miscibility of a CO₂/n-decane system”,Chinese Physics Letters,28, 0964011-0964014(2011)
12. H. Luo, D. Salama, S. Kryuchkov, A. Kantzas, “The effect of volume changes due to mixing on diffusion coefficient determination in heavy oil and hydrocarbon solvent system”,the 2007 SPE Annual Technical Conference and Exhibition held in Anaheim, California,USA, 11 November(2007)
13. L. Song, A. Kantzas, J. Bryan,“Experimental measurement of diffusion coefficient of CO₂ in heavy oil using x-ray computed-assisted tomography under reservoir conditions”the Canadian Unconventional Resources & International Petroleum Conference held in Calgary, Alberta, Canada, 19 October (2010)

14. D. Salama, A. Kantzas, “Monitoring of diffusion of heavy oils with hydrocarbon solvents in the presence of sand”, the 2005 SPE International Thermal Operations and Heavy Oil Symposium held in Calgary, Alberta, Canada, 1 November (2005)
15. D.B. Fisher, A.K. Singhal, S.K. Das, J. Goldman, C. Jackson. “Use of magnetic resonance imaging and advanced image analysis as a tool to extract mass transfer information from a 2D physical model of the Vapex process”, the 2000 SPE/DOE improved oil recovery symposium held in Tulsa, Oklahoma, 3 April (2000)
16. A. K. Tharanivasan, C. Yang, Y. Gu, “Measurements of Molecular Diffusion Coefficients of Carbon Dioxide, Methane, and Propane in Heavy Oil under Reservoir Conditions”, *Energy & Fuels*, 20, 2509-2517(2006)
17. Zhaowen Li, Mingzhe Dong, “Experimental Study of Carbon Dioxide Diffusion in Oil-saturated Porous Media”, *Ind. Eng. Chem. Res.* 48, 9307-9317(2009)
18. Y.C. Zhao, Y.C. Song, “Visualization of CO₂ and oil immiscible and miscible flow processes in porous media using NMR micro-imaging”, *Petroleum Science*, 8, 183-193(2011)
19. U. Guerrero-Aconcha, A. Kantzas, “Diffusion of hydrocarbon gases in heavy oil and bitumen”, The 2009 SPE Latin American and Caribbean Petroleum Engineering Conference held in Cartagena, Colombia, 31 May-3 June(2009)
20. C. Chang, M. Chang, “Non-iteration estimation of thermal conductivity using finite volume method”, *Int Commun Heat Mass Transfer*, 33, 1013-1020(2006)
21. M. Jamialahmadi, M. Emadi, “Diffusion coefficients of methane in liquid hydrocarbons at high pressure and temperature”, *Journal of Petroleum Science and Engineering*. 53, 47-60(2006)

22. L. S. Wang, Z.X. Lang, T.M. Guo, Measurement and correlation of the diffusion coefficients of carbon dioxide in liquid hydrocarbons under elevated pressures. *Fluid Phase Equilibria*. 117, 64-372. (1996)
23. A.T. Grogan, V.W. Pinczewski, G. Ruskauff, F.M. Orr Jr, Diffusion of CO₂ at reservoir conditions: models and measurements. *SPE Reservoir Engineering*. 2, 93-102. (1988)
24. R. Islas-Juárez, F. Samanego-V., “Experimental Study of Effective Diffusion in Porous Media”, The 2004 SPE International Petroleum Conference in Mexico held in Puebla, Mexico, 8-9 November (2004)